Special Issue of the 6th International Congress & Exhibition (APMAS2016), Maslak, Istanbul, Turkey, June 1–3, 2016

Improvement of Surface Properties of Low Carbon Steel by Nitriding Treatment

F.Z. Benlahreche[a,*] and E. Nouicer[b]

[a]Processes Engineering Faculty, Constantine3 University, Constantine 25000, Algeria

[b]Physics Department, Exact Sciences Faculty, Constantine1 University, Constantine 25000, Algeria

This work aimed to improve the physicochemical properties of a low carbon steel C15 by a nitriding treatment in a salt bath at 580 °C. The micrographs of treated sample show that the nitriding treatment causes significant structural changes, it is allowed to delineate the nitriding layer. The X-ray diffraction and the Raman spectroscopy of the treated samples permitted to identify different nitrides ($Fe_{2-3}N$, Fe_4N) formed. The obtained hardness profile determines the nitriding depth. Potentiodynamic curves show that the corrosion current density of treated C15 is the 10 times lower than untreated specimen. The values of impedance parameters obtained after nitriding treatment indicate that the resistance values and exponent n increase, whereas the capacitance decreases. We concluded that the nitriding treatment is an effective method for improvement of the corrosion behavior and surface properties of the low alloy steel C15.

DOI: 10.12693/APhysPolA.131.20

PACS/topics: 81.65.Lp

1. Introduction

Nitriding is a thermochemical surface treatment used in steels and alloys to improve wear and friction properties by surface microstructure modification, while maintaining adequate substrate properties. Not only wear resistance is improved, but also corrosion and fatigue resistance may be increased by the same treatment [1–6]. Nitrogen diffusion modifies surface and near surface microstructure producing hard layers with altered mechanical properties [7–10]. The layer on the ion nitrided steel consists of two parts, compound layer and diffusion layer. The outer and thinner layer consists of mainly γ'-Fe_4N and/or ε-$Fe_{2,3}N$ inter-metallic phases. Therefore, it is commonly called as "compound layer". On the other hand, it is also referred to as "white layer" because of its white color after nital etch on the microscopy. Thickness and phase content of compound layer depend on the treatment parameters such as: composition, time, and temperature [3, 11].

Zagonel et al. [12] examined the effect of temperature on the microstructure of treated hot work tool steel (AISI H13) by plasma pulsed nitriding and its influence on the material hardness. The analysis of the hardness profile curves confirms the temperature activation diffusion of nitrogen. The relatively high activation energy obtained suggests a complex diffusion mechanism involving the precipitation of alloying nitrides observed by SEM studies, giving an important increasing hardness.

Elango [13] reported the technique of plasma nitriding and nitro carburizing of austenitic stainless steels AISI 316L, the layers formed during these treatments characterized by high hardness and wear resistance. The plasma nitriding and nitro carburizing on AISI 316L stainless steel were conducted at 400, 450, and 500 °C. After plasma treatment, it was observed that the layer thickness increases with temperature. X-ray diffraction indicates the presence of iron carbide and/or chromium and iron nitrides. The potentiodynamic polarization curves obtained in 3.5% NaCl solution show that corrosion resistance is higher for the samples treated at 400 °C relative to the untreated substrate. A change in the dominant corrosion mechanism was also observed after nitriding or nitro carburizing from localized pitting corrosion to general corrosion.

The effect of salt bath nitriding on surface properties like micro-hardness, corrosion resistance and wear resistance of AISI 316L was studied by Subbiah et al.[14]. The surface hardness increases with the diffusion time and reaches the value of 1410 Hv. It was found that post-oxidation has no significant effect on the hardness but improves the corrosion resistance in comparison with non-oxidized specimen.

In this investigation realized by Ozturk et al. [15] a ferritic stainless steel (X36CrMo17) was plasma nitrided at 52–540 °C for 1–18 h under various gas mixtures of N_2+H_2 in an industrial nitriding facility. The nitriding conditions with the gas composition $N_2/H_2 = 1$ produces the thickest nitrided layer (135 μm) with enhanced corrosion protection. The nanohardness of the surface layers increased by about a factor of three in comparison to that of the substrate material.

The influence of pulsed plasma post-oxidation process on crystalline phase's composition and corrosion performance of plasma nitrided AISI 4340 steel was evaluated by Guillén et al. [16]. Pulsed plasma nitriding improved the surface morphology of untreated sample. Plasma post-oxidation process of nitrided AISI 4340 steel promotes the occurrence of a surface constituted by a magnetite thin layer on a thicker nitrided layer. The oxidized layer

*corresponding author; e-mail: benlahreche_fatima@yahoo.fr

is characterized by presence of kind Fe4N and Fe3N iron nitrides. The corrosion performance of the samples exposed to a salt fog was significantly better in the case of the oxidized samples compared with nitrided samples.

In this study, C15 low-alloy steel was nitrided under a salt bath, many techniques such as: microhardness tester, optical microscopy, X-ray diffraction, Raman and electrochemical impedance spectroscopy were used in this investigation.

2. Material and experimental techniques

2.1. Material

The experimental material was C15 low alloy steel. The specimens were 12 mm in diameter and 5 mm in thickness. Previous nitriding treatment, samples were ground using different grades of SiC emery paper (320, 400, 600, 800, 1000, 1200 progressively) and polished with a 0.5 μm diamond suspension. After that, specimens were cleaned ultrasonically, rinsed and dried, with care taken to avoid further fingers contact. The nitriding treatment was performed in a salt bath at a temperature of 580 °C for 6 h according the TENIFER process (TF1). The chemical compositions of the steel were given in Table I.

TABLE I

Chemical compositions of C15 low alloy steel.

element	C	Si	Mn	P	S	Cr	Ni	Mo
content [%]	0.18	0.43	0.45	0.012	0.017	0.10	0.10	0.01

2.2. Experimental techniques

Cyclic polarization measurements and impedance were performed in a glass cell with three electrodes: a working electrode, a platinum counter electrode and a saturated calomel reference electrode (SCE). The electrolyte was 3 wt% NaCl in double-distilled water.

The electrochemical measurements were conducted using a potentiostat type EG&G Model 283, combined with a frequency response analyzer, Model 1025, controlled by computer. The polarization curves were performed using the software Soft CorrIII. The impedance diagrams were obtained using the Power Suite software. The frequency range is between 10^{-2} Hz and 10^{5} Hz.

The nitrided layer was observed using optical microscope, after Nital 4% etching. Microhardness measurements were performed on a Vickers machine using a 300 g load. The X-ray diffraction and Raman spectroscopy were used for the nitrided surface characterization.

3. Results and discussion

3.1. Metallographic characterization

Microscopic observations allowed determining the nitriding layer as seen in Fig. 1 in the photographs we distinguish two zones: a high-contrast zone (white layer) that represents the compound layer and a less contrasted zone representing the diffusion layer.

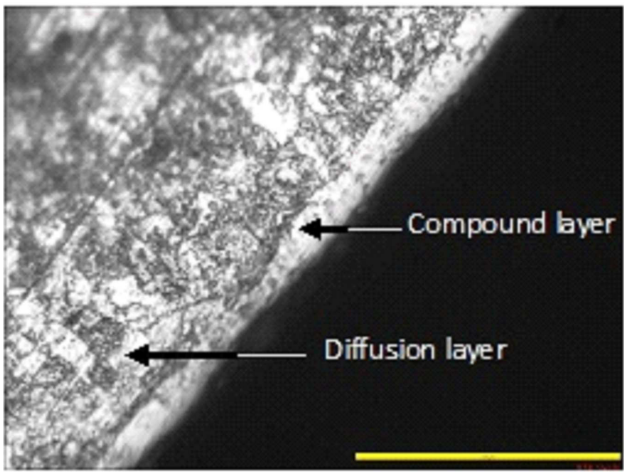

Fig. 1. Micrograph of C15 nitrided steel.

3.2. X-ray diffraction and Raman spectroscopy characterization

Figure 2 shows the X-ray diffraction patterns of the untreated and nitrided C15 low alloy steel. Figure 2 shows that the structure of untreated specimen is consisting of ferrite α (body centered cubic). The XRD results of nitrided specimens clearly show the formation of iron nitrides (labeled ε and γ'). The ε ($Fe_{2-3}N$) is the richest phase in nitrogen, its structure is hexagonal with an average of 2 or 3 nitrogen atoms in insertion. The γ' (Fe_4N) phase corresponds to face centered cubic, these two phases formed the compound layer (white layer) located in the surface front followed by diffusion layer.

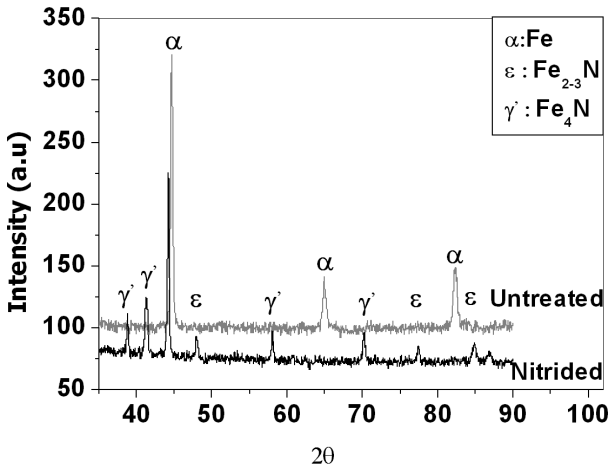

Fig. 2. XRD of C15 steel before and after nitriding.

The Raman spectra of untreated and nitrided specimens are shown in Fig. 3, the spectra show the iron nitrides $Fe_{2-3}N$ and Fe_4N formed during this process, we note that the most intense peaks corresponding to the α phase (ferrite) of substrate. These results are in good agreement with the obtained results by X-ray diffraction.

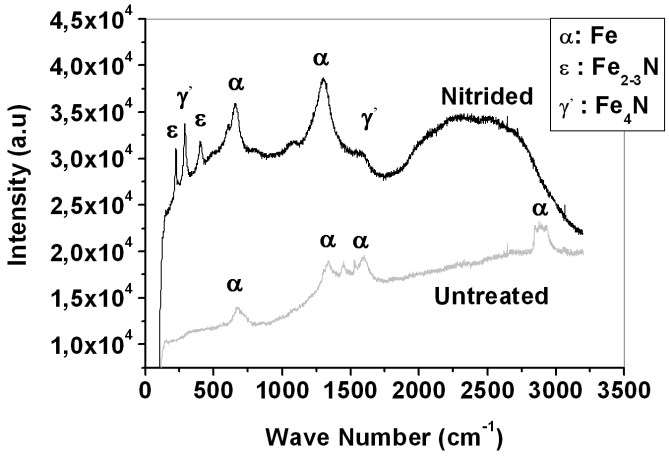

Fig. 3. Raman spectrum of C15 treated steel.

3.3. Microhardness characterization of c15 nitrided steel

In order to mechanically characterize the quality of the layer, microhardness tests were performed. These tests consist of performing HV Vickers microhardness tests under a load of 300 g, from the surface to the core on a cross-section of specimen [7]. The hardness decreases from surface to core. Indeed, the applied surface treatment has led to a structural hardening. The hardness profile as a function of depth is shown in Fig. 4.

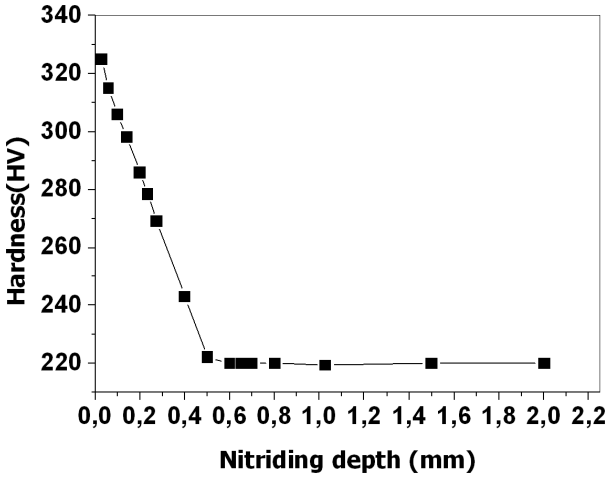

Fig. 4. Microhardness profile of C15 steel.

3.4. Cyclic polarization

Figure 5 shows a polarization curves plotted in the semilogarithmic scale, a slight shift of the corrosion potential of nitrided C15 low alloy steel in the more noble direction from –568 to –560 mV (saturated calomel electrode, SCE). The corrosion current densities of treated and untreated specimen are respectively 3.5 and 33 μA/cm^2. We note that the corrosion current density of treated C15 is of the order of 10 times lower than untreated. It is clear that the corrosion behavior is considerably improved.

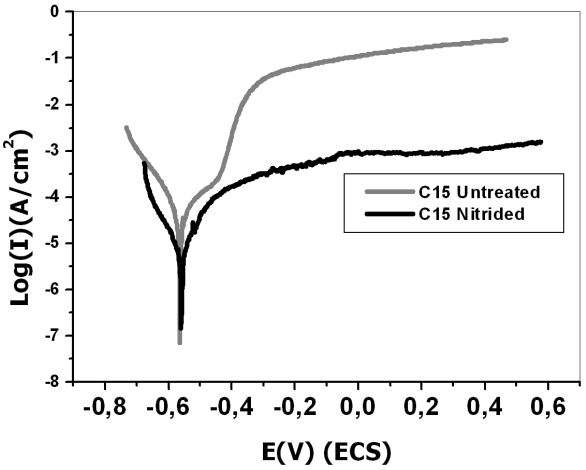

Fig. 5. Potentiodynamic curves of C15 steel in 3% NaCl solution before and after nitriding treatment.

3.5. Electrochemical impedance spectroscopy analysis

The electrochemical impedance spectroscopy (EIS) is another effective technique in the electrochemical characterization. The Nyquist and Bode diagrams were plotted before and after treatment. As shown in Fig. 6, the system behavior is not purely capacitive and so it is necessary to take into consideration the constant phase element Z (CPE) that represents the deviation compared with a purely capacitive behavior.

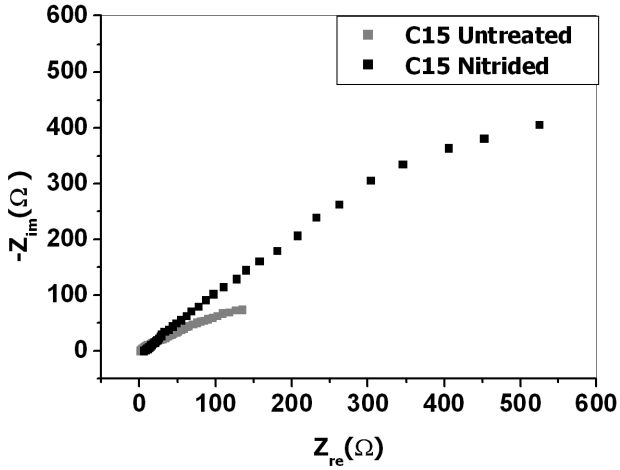

Fig. 6. Nyquist diagram of C15 steel in 3% NaCl solution before and after nitriding treatment.

TABLE II

Electrical parameters of the equivalent circuit obtained by fitting the experimental results of EIS.

C15	R_e [Ωcm^2]	R_t [Ωcm^2]	Q [mΩ^{-1}s^{n}cm^{-2}]	n
untreated	1.75	228.5	15.30	0.40
nitrided	4.71	1922	6.62	0.52

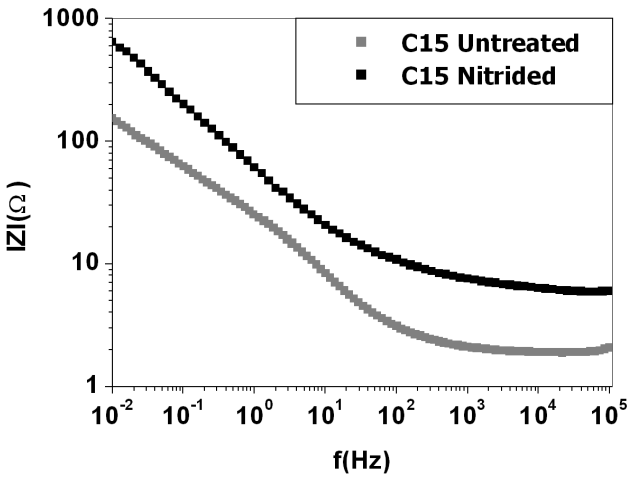

Fig. 7. Bode diagram of C15 steel in 3% NaCl solution before and after nitriding treatment.

The Nyquist diagrams presented in Fig. 6 show only a simple loop, a semicircle, indicating that the equivalent electrical circuit of the C15 (treated and untreated)/3% NaCl interface is similar to a resistance R_e of the electrolyte in series with CPE, which is in parallel with the corrosion resistance (R_t).

From Fig. 6, the nitriding treatment caused an increase in R_t. The larger the capacitive loop, the higher the corrosion resistance.

Bode plots (log|impedance| versus log|frequency|) is represented in Fig. 7. These plots have a linear pattern at middle frequencies with n values of 0.40 and 0.52 of treated and untreated C15, respectively. The increasing in n value related to the formation of compound layer during nitriding process.

The values of impedance parameters obtained by Zview software given in Table II indicate that the resistance values and exponent n increase after nitriding treatment, whereas the capacitance decreases.

4. Conclusion

This work aimed to improve the physical and chemical behaviour of C15 low alloy steel undergone nitriding treatment.

Microscopic observations allowed defining the nitriding layer. The X-ray analysis and Raman spectroscopy of the treated samples enabled to identify the different iron nitrides ($Fe_{2-3}N$, Fe_4N) formed. The Vickers microhardness tests were conducted. The treatment leads to an increase of the surface hardness compared with that of the matrix as a consequence the formation of iron nitrides.

The polarization curve and the impedance diagram showed a clear increase of the corrosion resistance of C15 nitriding. We conclude that nitriding is an effective method of surface treatment to improve the mechanical and electrochemical behavior of C15 low alloy steel, increasing the nitrogen content by direct diffusion through the surface, while keeping the unchangeable and tenacious heart that to absorb deformation and shocks.

References

[1] C.E. Pinedo, W.A. Monteiro, *J. Mater. Sci. Lett.* **20**, 147 (2001).

[2] A. Alsaran, M. Karakan, A. Celik, *Mater. Character.* **48**, 323 (2002).

[3] S.Y. Sirin, E. Kaluc, *Mater. Des.* **36**, 741 (2012).

[4] A. Ekinci, A. Akdemir, M.T. Demirci, in: *Proc. 6th Int. Advanced Technologies Symp. (IATS'11)*, Elazığ 2011, p. 431.

[5] I. Altinsoy, K.G. Onder, F.G. Celebi Efe, C. Bindal, *Acta Phys. Pol. A* **125**, 1249 (2014).

[6] A. de la Piedad-Beneitez, A.E. Muñoz-Castro, R. Valencia-Alvarado, R. López-Callejas, A. Mercado-Cabrera, R. Peña-Eguiluz, B. Rodriguez-Mendez, S.R. Barocio, *Acta Phys. Pol. A* **123**, 904 (2013).

[7] C. Allen, C.X. Li, T. Bell, Y. Sun, *Wear* **254**, 1106 (2003) .

[8] K. Genel, M. Demirkol, M. Capa, *Mater. Sci. Eng. A* **279**, 207 (2000).

[9] J.H. Sung, J.H. Kong, D.K. Yoo, H.Y. On, D.J. Lee, H.W. Lee, *Mater. Sci. Eng. A* **489**, 38 (2008).

[10] S.H. Yeh, L.H. Chiu, H. Chang, *Adv. Mater. Res.* **47-50**, 686 (2008).

[11] S.H. Yeh, L.H. Chiu, H. Chang, *Engineering* **3**, 942 (2011).

[12] L.F. Zagonel, C.A. Figueroa, R. Droppa Jr, F. Alvarez, *Surf. Coat. Technol.* **201**, 452 (2006).

[13] P. Elango, *Int. J. Eng. Res. Rev.* **2**, 18 (2014).

[14] R. Subbiah, S. Satheesh, S.C. Sunny, G. Kishor, K. Fahad, R. Rajavel, *Int. J. Innovat. Technol. Explor. Eng. IJITEE* **3**, 69 (2014) .

[15] O. Ozturk, O. Onmus, D.L. Williamson, *Surf. Coat. Technol.* **196**, 341 (2005).

[16] J.C. Díaz-Guillén, J.S. Zamarripa-Piña, E.E. Granda-Gutiérrez, M.A. González-Albarrán, J.A. Díaz-Guillén, S.I. Pérez-Aguilar, J. Candelas-Ramírez, *Int. J. Mod. Eng. Res. IJMER* **3**, 386 (2013).